Continuous One-Step Synthesis of Porous M-XF 6 -Based Metal-Organic and Hydrogen-Bonded Frameworks

Vincent Guillerm, Luis Garzón-Tovar, Amirali Yazdi, Inhar Imaz, Jordi Juanhuix, Daniel Maspoch

Continuous One-Step Synthesis of Porous M-XF6-based Metal-Organic and Hydrogen-Bonded Frameworks

Vincent Guillerm,[a] Luis Garzón-Tovar,[a] Amirali Yazdi,[a] Inhar Imaz,[a] Jordi Juanhuix[b] and Daniel Maspoch*[a],[c]*

[a] Catalan Institute of Nanoscience and Nanotechnology (ICN2), CSIC and The Barcelona Institute of Science and Technology, Campus UAB, Bellaterra, 08193 Barcelona, Spain. E-mail: inhar.imaz@icn2.cat, daniel.maspoch@icn2.cat

[b] ALBA Synchrotron Cerdanyola del Vallès, 08290 Barcelona, Spain

[c] ICREA, Pg. Lluís Companys 23, 08010 Barcelona, Spain

KEYWORDS: Metal-Organic Frameworks, Spray-Drying, CO_2 sorption, Stability, Fluorinated Materials

ABSTRACT

Metal-organic frameworks (MOFs) built up from connecting M-XF_6 pillars through N-donor ligands are among the most attractive adsorbents and separating agents for CO_2 and hydrocarbons today. Here, we show the continuous, one-step spray-drying synthesis of several members of this isoreticular MOF family varying the anionic pillar (X = $[SiF_6]^{2-}$ and $[TiF_6]^{2-}$), the N-donor organic

ligand (pyrazine and 4,4'-bipyridine) and the metal ion (M = Co, Cu and Zn). This synthetic method allows obtaining them in the form of spherical superstructures assembled from nanosized crystals. As confirmed by CO_2 and N_2 sorption studies, most of the M-XF_6-based MOFs synthesized via spray-drying can be considered "ready-to-use" sorbents as they do not need additional purification and time consuming solvent exchange steps to show comparable porosity and sorption properties than the bulk/single crystal analogues. Stability tests of nanosized M-SiF_6-based MOFs confirm their low stability in most of solvents, including water and DMF, highlighting the importance of protecting them once synthesized. Finally, we show for the first time that the spray-drying method can also be used to assembly hydrogen-bonded open networks, as evidenced by the synthesis of **MPM-1-TIFSIX**.

INTRODUCTION

The environmental impact associated to the energy demand is a major problem worldwide.[1] For example, CO2 emission caused by humanity - CO2 concentration at the South Pole recently passed the milestone of 400 ppm for the first time in the last 4 million years -[2] highly contributes to the climate change. In this sense, 2016 has also been the first year that the weekly CO2 concentration average monitored in the Mona Loa observatory did not go below this key value, meaning that the average global temperature is likely to increase more than the 1.5 oC warming threshold.[3]

To address the current and future energy needs while mitigating the environmental impact, one of the strategies has been the development of efficient CO2 capture, storage and separation materials for achieving cleaner combustible supplies.[4] These materials mainly include zeolites, activated carbons, metal-organic frameworks (MOFs) and covalent-organic frameworks (COFs).[5] Among these innovative materials, an old-fashioned class of fluorinated materials[6] have recently been

brought back to the spotlights by Eddaoudi and Zaworotko groups thanks to their exceptional uptake and selectivity towards CO2 and hydrocarbons.[7] These MOFs (Figure 1) are constructed from the assembly of pre-made M-XF6 pillars (M = Co, Ni, Cu, Zn; X = Si, Ti, Sn, Zr, Ge, V, Ga) with N-donor type ligands (e.g. pyrazine (pyz), pyridil-based ligands etc.).

However, despite these great developments, scientific community and industrials still need to join their efforts for transferring these materials from the laboratory to industry. A very important step here is the optimization of their fabrication.[8] This fabrication must always envision fast and scalable one-step processes that produce ready-to-use products without the need of additional purification and drying steps. Here we report a synthetic method that allows producing several of the isoreticular M-XF6-based CO_2 sorbents fulfilling all these requirements.

Our team recently introduced an industrially well-established spray-drying (SD) technique as a new synthetic way to prepare various MOFs (Scheme S1).[8l, 9] The SD technique is a scalable and fast method allowing continuous synthesis of MOFs in the form of spherical superstructures or beads based on the assembly of nanosized crystals.[9c] The strong expertise acquired from these previous studies, among several reports suggesting the capital importance of the formation of the inorganic secondary building unit (SBU) for the nucleation and growth of MOFs,[10] convinced us that premade pillars of the M-XF6 MOF platform would be ideal candidates for SD synthesis.

We therefore successfully embarked in the SD-based synthesis of several M-XF6 based materials, showing that this method is also compatible for reticular synthesis and metal tuning, ligand elongation and pillar substitution. Importantly, their rapid synthesis (few minutes versus few hours up to few days) does not negatively affect their sorption properties, demonstrating in most cases its ready-to-use character without the need of additional purification steps or time consuming,

repeated solvent exchange procedures. Moreover, we also demonstrate that SD can be used not only to synthesize porous materials based on coordination bonds but also based on hydrogen bonds.

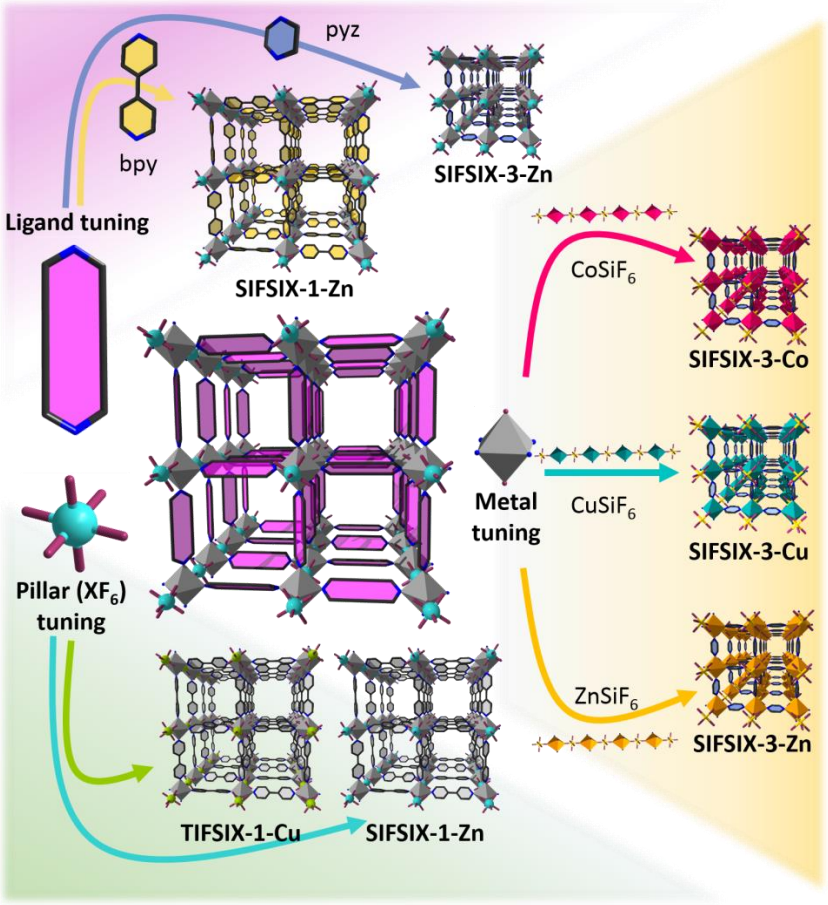

Figure 1. Schematic representation of the different isoreticular pcu M-XF6-based MOFs synthesized via spray-drying. Note here that this technique allows synthesizing this class of MOFs varying the metal ion (Co, Cu, Zn), anionic pillar ([SiF6]2-, [TiF6]2-) and ligand (pyrazine, 4,4'-bipyridine).

RESULTS AND DISCUSSION

SIFSIX-3-M Materials

Synthesis and characterization

The one-step SD synthesis consisted on the combined atomisation of two methanolic solutions containing (i) M-SiF6 (M = Co, Cu, Zn) and (ii) pyz at 85 oC, which produced fine powders that were collected with a minimum amount of methanol (MeOH). Collection of these powders in methanol was a crucial protection step as we found that they were air-sensitive (vide infra). To assess the quality of the as-made SIFSIX-3-M MOFs, their CO2 sorption properties were compared with those of their bulk analogues. For this, the SD-synthesized SIFSIX-3-M collected in methanol were directly transferred from the spray drier collector to sorption cells, and dried and evacuated for 12 h at 65 oC. Then, their CO2 uptake at 298 K was measured. Notably, we confirmed that spray-dried SIFSIX-3-M did not require additional solvent exchange or purification step to exhibit remarkable CO2 capacities at low pressure and 298 K (Figure 2h, Table 1), with an uptake less than 10 % lower than the reported bulk materials.

SD-synthesized SIFSIX-3-M were further characterised by powder X-ray diffraction (PXRD), from which experimental patterns were in excellent agreement with the theoretical diagrams calculated from the corresponding structures (Figure 2g), demonstrating both the high crystallinity and purity of the MOFs.

The morphology of the materials was also investigated by field-emission scanning electron microscopy (FE-SEM), showing in all cases the occurrence of nanosized SIFSIX-3-M crystals assembled into spherical superstructures or beads; a shape that is typical from MOFs assembled by the SD method. The sizes of these superstructures were 7.9 ± 4.8 μm for SIFSIX-3-Co, 6.9 ± 3.4 μm for SIFSIX-3-Cu, and 3.5 ± 2.7 μm for SIFSIX-3-Zn (Figure 2 a-c and Figure S14a).[9,

11] Moreover, FE-SEM images confirmed the homogeneity of the materials, as already suggested by the absence of crystalline impurity peaks in the PXRD diagrams.

To finally determine the size of crystals composing the superstructures, they were disassembled by sonication and immediately transferred to a transmission electron microscopy (TEM) grid. TEM images confirmed the formation of nanocrystals with a size of 32 ± 13 nm for SIFSIX-3-Co, 80 ± 12 nm for SIFSIX-3-Cu, and 28 ± 9 nm for SIFSIX-3-Zn (Figure 2d-f and Figure S14b).

Table 1 Comparison of the CO2 uptakes (760 torr, 298 K) in spray-dried and bulk SIFSIX-3-M MOFs.

	CO_2 uptake at 760 torr and 298 K ($mmol.g^{-1}$)	
MOF	Bulk	Sprayed (% of bulk)
SIFSIX-3-Co	≈ 2.79 [7k]	2.56 (92 %)
SIFSIX-3-Cu	≈ 2.40 [7b]	2.23 (93 %)
SIFSIX-3-Zn	≈ 2.46 [7a]	2.27 (91 %)

Stability in different media

The use of methanol to collect the fine powders produced with the SD method is capital to protect and use the as-made SIFSIX-3-M MOFs.[12] Without this precaution, all nanosized SIFSIX-3-M MOFs suffered a fast degradation and a loss of their CO2 sorption properties when they were exposed to ambient conditions. In addition, following the optimized washing procedure reported by Nugent et al.,[7a] we observed that the SD-synthesized SIFSIX-3-Zn was instantaneously solubilized upon addition of N,N-dimethylformamide (DMF), leading to a clear solution. Re-spray drying attempts of this clear solution did not allow re-assembling the SIFSIX-3-Zn framework. Instead, colourless single crystals (versus the yellow colour of SIFSIX-3-Zn crystals) appeared in the DMF solution after a period of ca. a month. This unknown structure, which crystallizes in P-1 space group, was solved by single crystal X-ray diffraction and appeared to be a cationic 1D coordination polymer with formula {[Zn(pyz)2(DMF)2(H2O)2].[SiF6]} (1). This structure results from the replacement of all SiF6 pillars and half of the pyz ligand by DMF and water molecules (Table S1, Figures S15-19). The positive charge of this coordination polymer [Zn(pyz)2(DMF)2(H2O)2]2+ is balanced by [SiF6]2- anions.

It is important to mention here that a similar behaviour was found when immersing SIFSIX-3-Zn in water, also leading to a complete solubilisation of the crystals. The incubation of nanosized SIFSIX-3-Zn in other organic solvents, including acetonitrile, hexane, dichloromethane, chloroform, toluene, tetrahydrofuran and acetone, did not result in the solubilisation of the crystals but a fast phase transition into unidentified crystalline powders (Figure S20).

The only tested solvent in which SIFSIX-3-Zn showed certain stability was MeOH. Initial incubation studies using microcrystals instead of nanocrystals -to easily follow the evolution by FE-SEM- showed that SIFSIX-3-Zn is also etched and finally solubilized in MeOH (Figure S13). However, we found that the minimum amount of MeOH needed for the complete solubilisation of

the nanosized SIFSIX-3-Zn without stirring was around 0.14 mLMeOH per mg SIFSIX-3-Zn. In addition, below this amount of MeOH, SIFSIX-3-Zn remained stable and did not suffer any phase transition, as confirmed by PXRD. It is also worth to mention that a similar behaviour occurred for the Cu and Co analogues. To this end, altogether these observations allowed defining MeOH as the best solvent to collect these materials, which were in all cases collected using no more than 0.015 mLMeOH per mg of MOF.

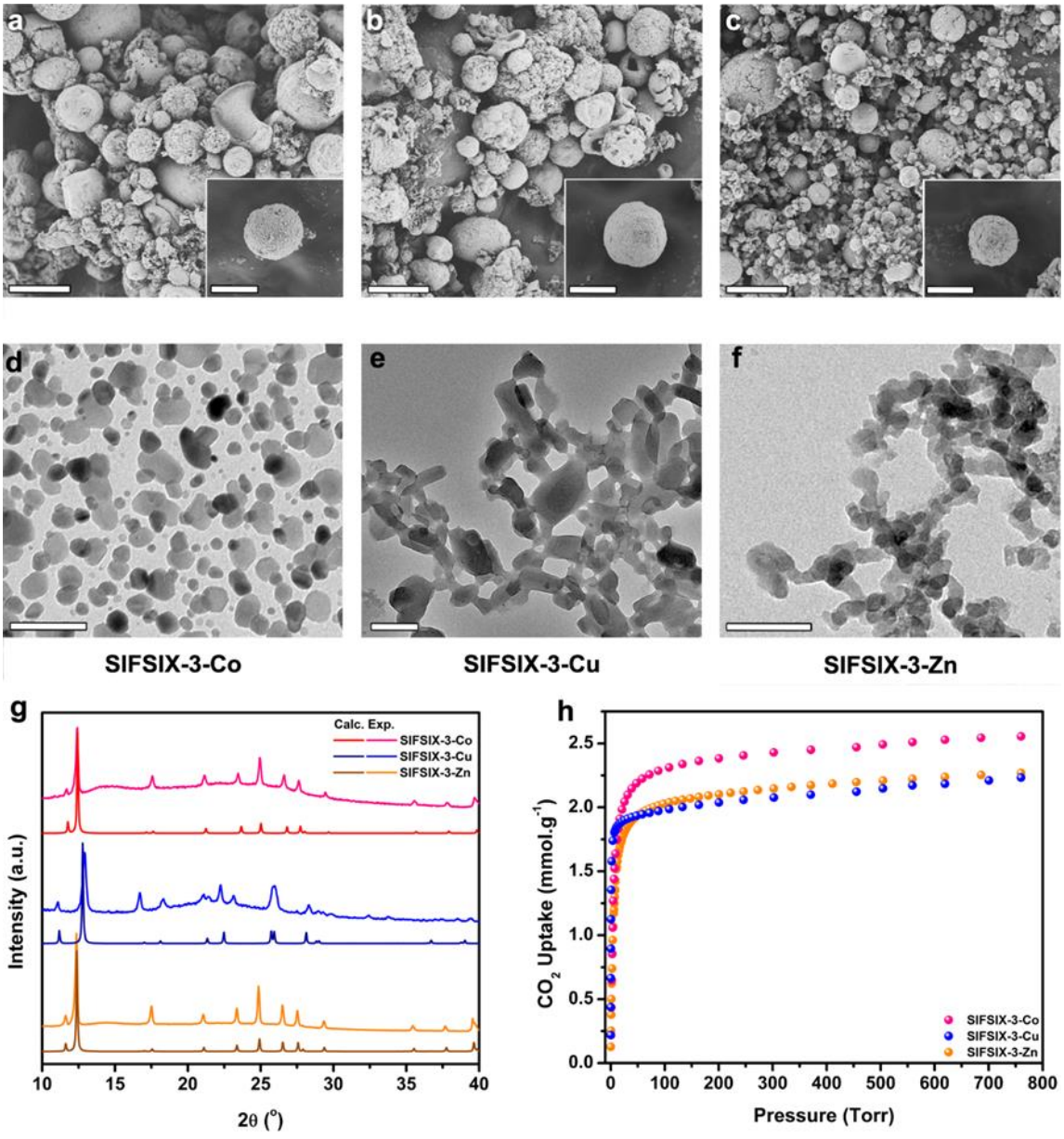

Figure 2. Representative FE-SEM images of (a) SIFSIX-3-Co, (b) SIFSIX-3-Cu, and (c) SIFSIX-3-Zn. TEM images of (d) SIFSIX-3-Co, (e) SIFSIX-3-Cu, and (f) SIFSIX-3-Zn. (g) PXRD diagrams of the SD-synthesized SIFSIX-3-M. (h) CO2 sorption isotherms at 298 K for SIFSIX-3-M. Scale bars for FE-SEM: 15 µm and 5 µm (insets). Scale bars for TEM: 100 nm (d, f) and 200 nm (e).

Reticular chemistry: organic ligand and anionic pillar tuning

Synthesis and characterization of SIFSIX-1-Zn. In line with global efforts of the "MOF community" to use some network topologies as design platforms to rationally synthesize isoreticular MOFs,[13] we intended to take advantage of the already reported versatility of the M-XF6 platform[6c, 6e, 7a, 7b, 7e-g, 7k] to demonstrate the suitability of the SD method for reticular chemistry. Following the successful synthesis of SIFSIX-3-M (M = Co, Cu and Zn), we successfully achieved the synthesis of an expanded analogue, SIFSIX-1-Zn,[6e] by replacing the pyz ligand by the longer 4,4'-bipyridine (bpy). Here, a methanolic solution of ZnSiF6 was spray-dried along with a methanolic solution of bpy using a 3-fluid nozzle at 85 oC. The resulting yellow spherical superstructures (size = 7.9 ± 3.6 µm; Figure 3c and Figure S14a) were collected and washed with MeOH. The material was obtained as a pure phase, as confirmed by PXRD (Figure 3b). Also, it was found to be porous to N2 at 77 K, exhibiting an apparent BET area of 1300 m2.g-1 (Table 2, Figure S21). Again, the nanosized nature of the SIFSIX-1-Zn crystals was confirmed by TEM performed after disassembling the superstructures by sonication. The size of these nanocrystals was 20 ± 5 nm (Figures S14b, S24).

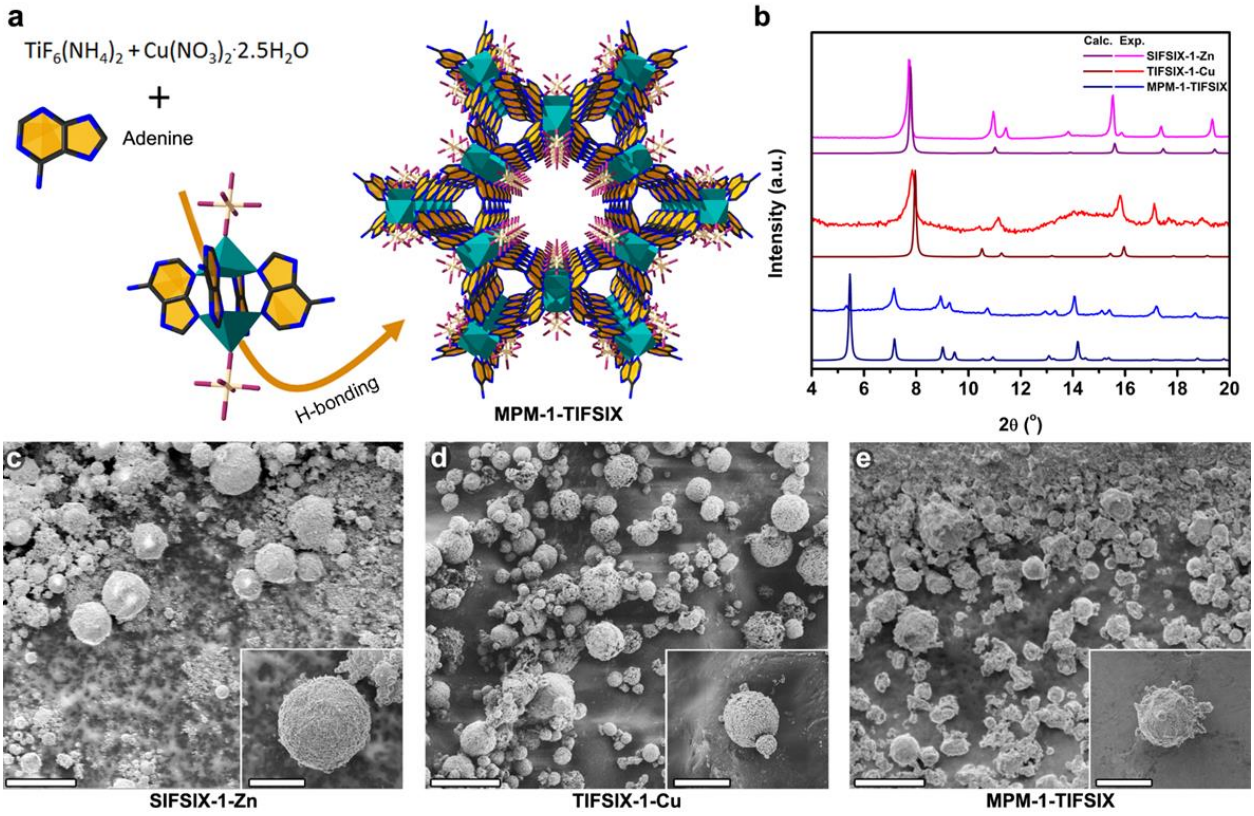

Figure 3. Schematic for the synthesis and structure of MPM-TIFSIX-1 (a); comparison of theoretical and experimental PXRD diagrams of MPM-1-TIFSIX, TIFSIX-1-Cu and SIFSIX-1-Zn (b); FE-SEM images of SIFSIX-1-Zn (c), TIFSIX-1-Cu (d) and MPM-1-TIFSIX (e). Scale bars for FE-SEM: 20 µm and 5 µm (insets).

Synthesis and characterization of TIFSIX-1-Cu

Recently, Nugent *et al*.[7f] reported the possibility to not only vary the metal in this type of **pcu**-MOFs, by achieving the replacement of the pillaring $[SiF_6]^{2-}$ anion by $[TiF_6]^{2-}$. Bulk **TIFSIX-1-Cu** is commonly synthesized using a layering of methanol and ethylene glycol at room temperature. However, this synthesis could not be reproduced in the spray-drier due to the high boiling point of ethylene glycol (197.3 °C). For this reason, we successfully replaced ethylene glycol by water, adjusting the SD temperature to 150 °C. Thus, an aqueous solution of

$Cu(NO_3)_2 \cdot 2.5(H_2O)$ and $TiF_6(NH_4)_2$ was spray-dried along with a methanolic solution of bpy using a 3-fluid nozzle at 150 °C. The resulting grey/purple spherical superstructures (size = 5.3 ± 3.1 μm; Figure 3d and Figure S14a) were collected with MeOH. Their PXRD diagram was found to be in excellent agreement with the theoretical diagram (Figure 3b). N_2 sorption performed at 77 K revealed an apparent BET area of 1650 $m^2.g^{-1}$. This value is very similar to that reported for the bulk material (1690 $m^2.g^{-1}$)[7f] demonstrating the high quality of the SD-synthesized **TIFSIX-1-Cu** MOF (Table 2, Figure S22). The nanosized nature of the **TIFSIX-1-Cu** crystals (size = 43 ± 9 nm, Figures S14b, S25) was again confirmed by TEM performed after disassembling the superstructures by sonication.

Synthesis and characterization of supramolecular open material

Finally, due to the apparent ease of synthesis of these M-XF6 based MOFs by SD technology, we selected another porous material, MPM-1-TIFSIX,[7d] based on the supramolecular assembly of [Cu2(ade)4(TiF6)2] (ade = adenine) paddlewheels (Figure 3a). It is worth to mention that, in the present case, the selected material to be synthesized by SD was not a MOF but a supramolecular hydrogen-bonded network. To our knowledge, the aerosol synthesis of such kind of open materials based on weak bonding has not been reported yet.

Table 2 BET areas and pore volumes for SIFSIX-1-Zn, TIFSIX-1-Cu and MPM-1-TIFSIX (N2, 77K).

MOF	A_{BET} ($m^2.g^{-1}$)	V_{micro} ($cm^3.g^{-1}$) at $P/P_0 = 0.3$	V_t ($cm^3.g^{-1}$) at $P/P_0 = 0.95$	Theo V_t ($cm^3.g^{-1}$)
SIFSIX-1-Zn	1300	0.53	0.58	0.68
TIFSIX-1-Cu	1650	0.66	0.88	0.70
MPM-1-TIFSIX	805	0.32	0.32	0.39

An aqueous solution of $Cu(NO_3)_2 \cdot 2.5(H_2O)$ and $TiF_6(NH_4)_2$ was spray-dried along with a solution of adenine in water/acetonitrile mixture using a 2-fluid nozzle (Scheme S3) at 150 °C. The resulting grey/purple spherical superstructures (size = 6.1 ± 3.1 μm; Figure 3e and Figure S14a) were collected with MeOH. Remarkably, the PXRD diagram was found to be in excellent agreement with the theoretical one (Figure 3b). N_2 sorption performed at 77 K after methanol solvent exchange procedure revealed an apparent BET area of 805 $m^2.g^{-1}$ (996 $m^2.g^{-1}$ for bulk),[7d] demonstrating the porosity of the SD-synthesized **MPM-1-TIFSIX** supramolecular material (Table 2, Figure S3). In this case, TEM experiments performed after disassembling the superstructures by sonication showed **MPM-1-TIFSIX** crystals with a size of 201 ± 65 nm (Figures S14b, S26).

CONCLUSION

We reported here the one-step and continuous synthesis of various M-XF6 based MOFs using the SD technique. Using this method, these M-XF6 based MOFs could be synthesized at the nanoscale. There is no doubt that the possibility of obtaining and stabilizing nanosized M-XF6

based MOFs opens new avenues on the re-exploration of this old-fashioned sub-class of MOFs for emerging applications. In addition, we demonstrated the suitability of the SD method to perform fine structural tuning via ligand size variation (pyz versus bpy), anionic pillar substitution ([SiF6]2- versus [TiF6]2-), and variation of metal ion (Co, Cu, and Zn). Importantly, this novel way to synthesize these materials does not jeopardize their sorption properties. This fact together with the short synthesis times and the absence of time consuming purification and solvent exchange procedures demonstrates the ability and competitiveness of SD methods versus conventional ones for the fast production of ready-to-use sorbents. Finally, we anticipate the first aerosol synthesis of a supramolecular, hydrogen bonded porous network, MPM-1-TIFSIX, which opens new avenues for the synthesis of this class of porous materials using SD.

EXPERIMENTAL SECTION

Materials

All the materials were synthesized using a Mini Spray Dryer B-290 (BÜCHI Labortechnik). All solvents and reagents were purchased from Sigma-Aldrich, City Chemicals and Scharlab and used as received.

Synthesis of SIFSIX-3-Co

A 6 mL methanolic solution of 300 mg (1.49 mmol) of CoSiF6 and a 6 mL methanolic solution of 325 mg (4.05 mmol) of pyz were simultaneously spray-dried using a 3-fluid nozzle (Scheme S2), a feed rate of 2.4 mL.min-1, a flow rate of 414 mL.min-1, an inlet N2 temperature of 85 oC, and a spray cap with a 0.5 mm hole. The light pink powder of SIFSIX-3-Co was recovered with a minimum amount of methanol (MeOH) (235 mg; 44% yield based on Co). IR bands (cm-1): 690

(s), 1062 (s), 1124 (w), 1153 (m), 1421 (s), 1628 (m), 1660 (m), 3196 (br), 3403 (br), 3522 (w) (Figure S1).

Synthesis of SIFSIX-3-Cu

A 6 mL methanolic solution of 300 mg (1.34 mmol) of CuSiF6·H2O and a 6 mL methanolic solution of 325 mg (4.05 mmol) of pyz were simultaneously spray-dried using a 3-fluid nozzle, a feed rate of 2.4 mL.min-1, a flow rate of 414 mL.min-1, an inlet N2 temperature of 85 oC, and a spray cap with a 0.5 mm hole. The blue powder of SIFSIX-3-Cu was recovered with a minimum amount of MeOH (272 mg; 55% yield based on Cu). IR bands (cm-1): 686 (s), 822 (s) 1078 (s), 1132 (s), 1161 (s), 1429 (s), 1652 (m), 1660 (m), 3147 (m), 3325 (br) (Figure S2).

Synthesis of SIFSIX-3-Zn

A 6 mL methanolic solution of 300 mg (1.45 mmol, anhydrous based) of ZnSiF6·xH2O and a 6 mL methanolic solution of 325 mg (4.05 mmol) of pyz were simultaneously spray-dried using a 3-fluid nozzle, a feed rate of 2.4 mL.min-1, a flow rate of 414 mL.min-1, an inlet N2 temperature of 85 oC, and a spray cap with a 0.5 mm hole. The yellow powder of SIFSIX-3-Zn was recovered with a minimum amount of MeOH (305 mg; 57% yield based on Zn). IR bands (cm-1): 686 (s), 822 (w), 1062 (s), 1099 (w), 1128 (w), 1161 (w), 1425 (s), 1635 (s), 1660 (m), 3432 (br) (Figure S3).

Synthesis of SIFSIX-1-Zn

A 6 mL methanolic solution of 300 mg (1.45 mmol, anhydrous based) of ZnSiF6·xH2O and a 6 mL methanolic solution of 650 mg (4.16 mmol) of bpy were simultaneously spray-dried using a 3-fluid nozzle, a feed rate of 2.4 mL.min-1, a flow rate of 414 mL.min-1, an inlet N2 temperature

of 85 ºC, and a spray cap with a 0.5 mm hole. The yellow powder of SIFSIX-1-Zn was recovered with a minimum amount of MeOH (302 mg; 40 % yield based on Zn). Sample was then washed with 5 mL of MeOH to remove potential contamination with the highly soluble, unreacted precursors. IR bands (cm-1): 632 (m), 649 (s), 764 (m), 806 (s), 851 (s), 1008 (m), 1062 (s), 1223 (m), 1317 (w), 1413 (s), 1491 (m), 1536 (m), 1611 (s), 1644 (w), 3230 (w), 3345 (br) (Figure S4).

Synthesis of TIFSIX-1-Cu

A 6 mL aqueous solution of 30 mg (0.15 mmol) of TiF6·(NH4)2 and 35 mg (0.15 mmol) of Cu(NO3)2·2.5(H2O) and a 6 mL methanolic solution of 46.8 mg (0.30 mmol) of bpy were simultaneously spray-dried using a 3-fluid nozzle, a feed rate of 2.4 mL.min-1, a flow rate of 414 mL.min-1, an inlet N2 temperature of 130 oC, and a spray cap with a 0.5 mm hole. The blue powder of TIFSIX-1-Cu was recovered with a minimum amount of MeOH (64 mg; 79 % yield based on Cu). IR bands (cm-1): 632 (s), 678 (w), 728 (m), 810 (s), 851 (w), 921 (w), 1012 (s), 1066 (s), 1223 (m), 1280 (s), 1326 (w), 1409 (s), 1471 (m), 1491 (m), 1536 (m), 1607 (s), 1644 (w), 3101 (w), 3283 (w), 3357 (w) (Figure S5).

Synthesis of MPM-1-TIFSIX

A 12 mL aqueous solution of 30 mg (0.15 mmol) of TiF6·(NH4)2 and 35 mg (0.15 mmol) of Cu(NO3)2·2.5(H2O) and a 12 mL H2O:CH3CN (1:1 vol.) solution of 82 mg (0.60 mmol) of adenine were simultaneously spray-dried using a 2-fluid nozzle and T-shaped system (Scheme S3), a feed rate of 2.4 mL.min-1, a flow rate of 414 mL.min-1, an inlet N2 temperature of 150 oC, and a spray cap with a 0.5 mm hole. The purple/grey powder of MPM-1-TIFSIX was recovered with a minimum amount of MeOH (110 mg; 74% yield based on Zn). Prior to sorption measurements, this powder was immersed in MeOH for 3 days, refreshing the MeOH twice a day.

IR bands (cm-1): 715 (m), 789 (m), 827 (w), 806 (s), 889 (m), 938 (m), 1037 (w), 1107 (w), 1149 (w), 1231 (s), 1314 (s), 1409 (s), 1607 (s), 1652 (s), 1702 (w), 3089 (w), 3200 (w), 3419 (w) (Figure S6).

Characterization

PXRD diagrams were collected on a Panalytical X'pert diffractometer with monochromatic Cu-Kα radiation (λ_{Cu} = 1.5406 Å) under a Kapton film. Fourier transform infrared (FT-IR) spectra were recorded on a Bruker Tensor 27FTIR spectrometer equipped with a Golden Gate diamond attenuated total reflection (ATR) cell, in transmittance mode at room temperature. Main IR bands (Figures S1-6) are reported as follow: strong (s), medium (m), weak (w) and broad (br). TGA curves (Figures S7-12) were carried out in a Perkin Elmer Pyris 1 under O2 atmosphere and a heating rate of 10 $^{o}C.min^{-1}$. Volumetric N_2 and CO_2 sorption isotherms were collected at 77 K (N2) and 298 K (CO2) using an ASAP 2020 HD (Micromeritics). Temperature was controlled by using a liquid nitrogen bath (77 K) or a Lauda Proline RP 890 chiller (298 K). For N2 sorption at 77 K, micropore volumes (Vmicro) were calculated at P/P0 = 0.3, whereas the total pore volumes (Vt) were calculated at P/P0 = 0.95. Field-emission scanning electron microscopy (FE-SEM) images were collected on scanning electron microscopes (FEI Magellan 400L XHR and Quanta 650 FEG) at acceleration voltage of 1.0 kV, and using dry powder on carbon as support. Transmission electron microscopy (TEM) images were obtained with a JEOL JEM 1400 at 100 kV. Prior to TEM, all superstructures immersed in MeOH were disassembled by sonication for 10 s in a Fisher Scientific FB15051 sonicator and then, directly transferred on the TEM grids. Average size range of superstructures and crystals has been calculated on 100 crystals/superstructures using the Image J software.

Stability study of SIFSIX-3-Zn

A 6 mL methanolic solution of 300 mg (1.45 mmol, anhydrous based) of ZnSiF6·xH2O was injected to a 6 mL methanolic solution of 325 mg (4.05 mmol) of pyz at room temperature, without stirring. After 1 h, 1 mL of the solution containing the resulting microcrystals was pipetted from the middle of the vial and mixed with 2 mL of MeOH. Aliquots of the sample were transferred immediately to the microscope to avoid contact with air, and the morphology of the crystals was studied by FE-SEM after 15 min (Figure S13).

Crystallography

Crystallographic data for 1 were collected at 100 K at XALOC beamline at ALBA synchrotron[14] ($\lambda = 0.79472$ Å). Data were indexed, integrated and scaled using the XDS program.[15] Absorption correction was not applied. The structure was solved by direct methods and subsequently refined by correction of F2 against all reflections, using SHELXS2013[16] and SHELXL2013[17] within the WinGX package.[18] All non-hydrogen atoms were refined with anisotropic thermal parameters by full-matrix least-squares calculations on F2 using the program SHELXL2013. Hydrogen atoms were inserted at calculated positions and constrained with isotropic thermal parameters.

ASSOCIATED CONTENT

Supporting Information.

AUTHOR INFORMATION

Corresponding Author

* E-mail: inhar.imaz@icn2.cat, daniel.maspoch@icn2.cat

Notes

There are no conflicts to declare.

ACKNOWLEDGMENT

This work was supported by the MINECO-Spain through projects PN MAT2012-30994, 2014-SGR-80, EU FP7 ERC-Co 615954, and European Union's Horizon 2020 research and innovation programme under grant agreement No 685727. V.G. is grateful to the Generalitat de Catalunya for a Beatriu de Pinós fellowship (2014 BP-B 00155) and I.I. thanks the MINECO for a Ramón y Cajal fellowship (RYC-2010-06530). A.Y. and ICN2 acknowledge the support of the Spanish MINECO through the Severo Ochoa Centers of Excellence Program, under Grant SEV-2013-0295.

REFERENCES

1. [1] R. Monastersky, Nature 2009, 458, 1091-1094.

[2] South Pole is the last place on Earth to pass a global warming milestone, http://research.noaa.gov/News/NewsArchive/LatestNews/TabId/684/ArtMID/1768/ArticleID/11760/South-Pole-is-the-last-place-on-Earth-to-pass-a-global-warming-milestone.aspx, (accessed June 28th, 2016).

[3] Up-to-date weekly average CO2 at Mauna Loa, http://www.esrl.noaa.gov/gmd/ccgg/trends/weekly.html, (accessed October 4th, 2016).

[4] a) K. Sumida, D. L. Rogow, J. A. Mason, T. M. McDonald, E. D. Bloch, Z. R. Herm, T.-H. Bae, J. R. Long, Chem. Rev. 2012, 112, 724-781; b) Y. Belmabkhout, V. Guillerm, M. Eddaoudi, Chem. Eng. J. 2016, 296, 386-397.

[5] a) H. C. Zhou, J. R. Long, O. M. Yaghi (Ed), in Chem. Rev., Vol. 673-1268, 2012, p. 112; b) J. R. Long, O. M. Yaghi, in Chem. Soc. Rev., Vol. 1201-1508, 2009, p. 38; c) J. R. Long, O. M. Yaghi, in Chem. Soc. Rev., Vol. 5415-6172, 2014, p. 43; d) R. Dawson, A. I. Cooper, D. J. Adams, Prog. Polym. Sci. 2012, 37, 530-563.

[6] a) K. Uemura, A. Maeda, T. K. Maji, P. Kanoo, H. Kita, Eur. J. Inorg. Chem. 2009, 2009, 2329-2337; b) D. N. Dybtsev, H. Chun, K. Kim, Angew. Chem. Int. Ed. 2004, 43, 5033-5036; c) S.-I. Noro, S. Kitagawa, M. Kondo, K. Seki, Angew. Chem. Int. Ed. 2000, 39, 2081-2084; d) M. J. Zaworotko, Angew. Chem. Int. Ed. 2000, 39, 3052-3054; e) S. Subramanian, M. J. Zaworotko, Angew. Chem. Int. Ed. 1995, 34, 2127-2129; f) S.-I. Noro, R. Kitaura, M. Kondo, S. Kitagawa, T. Ishii, H. Matsuzaka, M. Yamashita, J. Am. Chem. Soc. 2002, 124, 2568-2583; g) M.-J. Lin, A. Jouaiti, N. Kyritsakas, M. W. Hosseini, CrystEngComm 2009, 11, 189-191.

[7] a) P. Nugent, Y. Belmabkhout, S. D. Burd, A. J. Cairns, R. Luebke, K. Forrest, T. Pham, S. Ma, B. Space, Ł. Wojtas, M. Eddaoudi, M. J. Zaworotko, Nature 2013, 495, 80-84; b) O. Shekhah, Y. Belmabkhout, Z. Chen, V. Guillerm, A. Cairns, K. Adil, M. Eddaoudi, Nature Commun. 2014, 5, 4228; c) P. Kanoo, S. K. Reddy, G. Kumari, R. Haldar, C. Narayana, S. Balasubramanian, T. K. Maji, Chem. Commun. 2012, 48, 8487-8489; d) P. S. Nugent, V. L. Rhodus, T. Pham, K. Forrest, Ł. Wojtas, B. Space, M. J. Zaworotko, J. Am. Chem. Soc. 2013, 135,

10950-10953; e) O. Shekhah, Y. Belmabkhout, K. Adil, P. M. Bhatt, A. J. Cairns, M. Eddaoudi, Chem. Commun. 2015, 51, 13595-13598; f) P. Nugent, V. Rhodus, T. Pham, B. Tudor, K. Forrest, Ł. Wojtas, B. Space, M. Zaworotko, Chem. Commun. 2013, 49, 1606-1608; g) S. D. Burd, S. Ma, J. A. Perman, B. J. Sikora, R. Q. Snurr, P. K. Thallapally, J. Tian, Ł. Wojtas, M. J. Zaworotko, J. Am. Chem. Soc. 2012, 134, 3663-3666; h) X. Cui, K. Chen, H. Xing, Q. Yang, R. Krishna, Z. Bao, H. Wu, W. Zhou, X. Dong, Y. Han, B. Li, Q. Ren, M. J. Zaworotko, B. Chen, Science 2016, 353, 141-144; i) A. Cadiau, K. Adil, P. M. Bhatt, Y. Belmabkhout, M. Eddaoudi, Science 2016, 353, 137-140; j) J. L. Manson, J. A. Schlueter, K. E. Garrett, P. A. Goddard, T. Lancaster, J. Moeller, S. J. Blundell, A. J. Steele, I. Franke-Chaudet, F. L. Pratt, J. Singleton, J. Bendix, S. H. Lapidus, M. Uhlarz, O. Ayala-Valenzuela, R. McDonald, M. Gurak, C. Baines, Chem. Commun. 2016; k) S. K. Elsaidi, M. H. Mohamed, H. T. Schaef, A. Kumar, M. Lusi, T. Pham, K. A. Forrest, B. Space, W. Xu, G. J. Halder, J. Liu, M. J. Zaworotko, P. K. Thallapally, Chem. Commun. 2015, 51, 15530-15533.

[8] a) P. Silva, S. M. F. Vilela, J. P. C. Tome, F. A. Almeida Paz, Chem. Soc. Rev. 2015, 44, 6774-6803; b) A. U. Czaja, N. Trukhan, U. Müller, Chem. Soc. Rev. 2009, 38, 1284-1293; c) U. Mueller, M. Schubert, F. Teich, H. Puetter, K. Schierle-Arndt, J. Pastre, J. Mater. Chem. 2006, 16, 626-636; d) M. Gaab, N. Trukhan, S. Maurer, R. Gummaraju, U. Müller, Micropor. Mesopor. Mater. 2012, 157, 131-136; e) D. Crawford, J. Casaban, R. Haydon, N. Giri, T. McNally, S. L. James, Chem. Sci. 2015, 6, 1645-1649; f) M. Rubio-Martinez, M. P. Batten, A. Polyzos, K.-C. Carey, J. I. Mardel, K.-S. Lim, M. R. Hill, Sci. Rep. 2014, 4, 5443; g) M. Rubio-Martinez, T. D. Hadley, M. P. Batten, K. Constanti-Carey, T. Barton, D. Marley, A. Mönch, K.-S. Lim, M. R. Hill, ChemSusChem 2016, 9, 938-941; h) P. A. Bayliss, I. A. Ibarra, E. Perez, S. Yang, C. C. Tang, M. Poliakoff, M. Schroder, Green Chem. 2014, 16, 3796-3802; i) M. Faustini, J. Kim, G.-Y. Jeong, J.

Y. Kim, H. R. Moon, W.-S. Ahn, D.-P. Kim, J. Am. Chem. Soc. 2013, 135, 14619-14626; j) P. W. Dunne, E. Lester, R. I. Walton, React. Chem. Eng. 2016, 1, 352-360; k) L. Garzón-Tovar, A. Carné-Sanchez, C. Carbonell, I. Imaz, D. Maspoch, J. Mater. Chem. A 2015, 3, 20819-20826; l) L. Garzón-Tovar, M. Cano-Sarabia, A. Carné-Sánchez, C. Carbonell, I. Imaz, D. Maspoch, React. Chem. Eng. 2016, 1, 533-539.

[9] a) Z. Wang, D. Ananias, A. Carné-Sánchez, C. D. S. Brites, I. Imaz, D. Maspoch, J. Rocha, L. D. Carlos, Adv. Funct. Mater. 2015, 25, 2824-2830; b) A. Carné-Sánchez, K. C. Stylianou, C. Carbonell, M. Naderi, I. Imaz, D. Maspoch, Adv. Mater. 2015, 27, 869-873; c) A. Carné-Sánchez, I. Imaz, M. Cano-Sarabia, D. Maspoch, Nature Chem. 2013, 5, 203-211.

[10] a) D. C. Cantu, B. P. McGrail, V.-A. Glezakou, Chem. Mater. 2014, 26, 6401-6409; b) O. Shekhah, H. Wang, D. Zacher, R. A. Fischer, C. Woll, Angew. Chem. Int. Ed. 2009, 48, 5038-5041; c) S. Surblé, F. Millange, C. Serre, G. Férey, R. I. Walton, Chem. Commun. 2006, 1518-1520; d) V. Guillerm, S. Gross, C. Serre, T. Devic, M. Bauer, G. Férey, Chem. Commun. 2010, 46, 767-769; e) D. Alezi, Y. Belmabkhout, M. Suyetin, P. M. Bhatt, Ł. J. Weseliński, V. Solovyeva, K. Adil, I. Spanopoulos, P. N. Trikalitis, A.-H. Emwas, M. Eddaoudi, J. Am. Chem. Soc. 2015, 137, 13308-13318.

[11] a) A. Garcia Marquez, P. Horcajada, D. Grosso, G. Férey, C. Serre, C. Sanchez, C. Boissière, Chem. Commun. 2013, 49, 3848-3850; b) A. Carné-Sánchez, I. Imaz, K. C. Stylianou, D. Maspoch, Chem. Eur. J. 2014, 20, 5192-5201.

[12] J. A. Mason, T. M. McDonald, T.-H. Bae, J. E. Bachman, K. Sumida, J. J. Dutton, S. S. Kaye, J. R. Long, J. Am. Chem. Soc. 2015, 137, 4787-4803.

[13] a) V. Guillerm, D. Kim, J. F. Eubank, R. Luebke, X. Liu, K. Adil, M. S. Lah, M. Eddaoudi, Chem. Soc. Rev. 2014, 43, 6141-6172; b) M. Eddaoudi, J. Kim, N. Rosi, D. Vodak, J. Wachter, M. O'Keeffe, O. M. Yaghi, Science 2002, 295, 469-472; c) O. M. Yaghi, M. O'Keeffe, N. W. Ockwig, H. K. Chae, M. Eddaoudi, J. Kim, Nature 2003, 423, 705-714; d) H. Furukawa, K. E. Cordova, M. O'Keeffe, O. M. Yaghi, Science 2013, 341; e) V. Guillerm, Ł. J. Weseliński, J., Y. Belmabkhout, A. J. Cairns, V. D'Elia, Ł. Wojtas, K. Adil, M. Eddaoudi, Nature Chem. 2014, 6, 673-680.

[14] J. Juanhuix, F. Gil-Ortiz, G. Cuni, C. Colldelram, J. Nicolas, J. Lidon, E. Boter, C. Ruget, S. Ferrer, J. Benach, J. Synchr. Rad. 2014, 21, 679-689.

[15] W. Kabsch, Acta. Crystallogr. Sect. D 2010, 66, 125-132.

[16] G. M. Sheldrick, Z. Dauter, K. S. Wilson, H. Hope, L. C. Sieker, Acta. Crystallogr. Sect. D 1993, 49, 18-23.

[17] G. M. Sheldrick, Acta. Crystallogr. Sect. C 2015, 71, 3-8.

[18] L. Farrugia, J. Appl. Crystallogr. 2012, 45, 849-854.